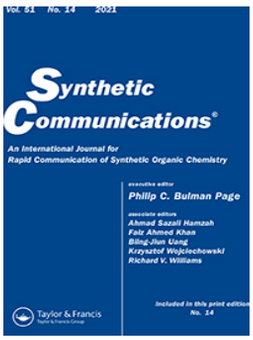

Taylor & Francis
Taylor & Francis Group

Synthetic Communications

An International Journal for Rapid Communication of Synthetic Organic Chemistry

ISSN: (Print) (Online) Journal homepage: https://www.tandfonline.com/loi/lsyc20

Efficient synthesis and molecular docking studies of new pyrimidine-chromeno hybrid derivatives as potential antiproliferative agents

Sevtap Çağlar Yavuz, Senem Akkoç, Burak Tüzün, Onur Şahin & Emin Saripinar

To cite this article: Sevtap Çağlar Yavuz, Senem Akkoç, Burak Tüzün, Onur Şahin & Emin Saripinar (2021) Efficient synthesis and molecular docking studies of new pyrimidine-chromeno hybrid derivatives as potential antiproliferative agents, Synthetic Communications, 51:14, 2135-2159, DOI: 10.1080/00397911.2021.1922920

To link to this article: https://doi.org/10.1080/00397911.2021.1922920

SYNTHETIC COMMUNICATIONS®
2021, VOL. 51, NO. 14, 2135–2159
https://doi.org/10.1080/00397911.2021.1922920

Taylor & Francis
Taylor & Francis Group

Efficient synthesis and molecular docking studies of new pyrimidine-chromeno hybrid derivatives as potential antiproliferative agents

Sevtap Çağlar Yavuz[a,b], Senem Akkoç[c], Burak Tüzün[d], Onur Şahin[e], and Emin Saripinar[a]

[a]Department of Chemistry, Faculty of Science, Erciyes University, Kayseri, Turkey; [b]Department of Veterinary Science, Şefaatli Vocational School, Yozgat Bozok University, Yozgat, Turkey; [c]Department of Basic Pharmaceutical Sciences, Faculty of Pharmacy, Süleyman Demirel University, Isparta, Turkey; [d]Department of Chemistry, Faculty of Science, Sivas Cumhuriyet University, Sivas, Turkey; [e]Scientific and Technological Research Application and Research Center, Sinop University, Sinop, Turkey

ABSTRACT

Various novel heterocyclic compounds containing pyrimidine nuclei 5*H*-chromeno[4,3-*d*]pyrimidine (**4a–c**, **e–h**, **l–r**, **t)** and pyrimidine-5-yl-(2-hydroxyphenyl)methanone (**5a**, **c**, **d**, **f–k**, **m–o**, **r**, **s**, **u)** were synthesized from the reaction of guanylhydrazones **(2a–u)** and 3-formylchromone **(3)**. These compounds were tested against human liver hepatocellular carcinoma cell line (HepG2) and human breast adenocarcinoma cell line (MDA-MB-231) using the MTT assay method. Furthermore, molecular docking calculations were performed to compare the biological activities of various novel heterocyclic compounds against cancer proteins. In these calculations, the protein used are crystal structure of the BRCT repeat region from the breast cancer associated protein, 1JNX, crystal structure of VEGFR kinase (liver cancer) protein, 3WZE, and crystal structure of an allosteric Eya2 phosphates inhibitor (lung cancer) protein, 5ZMA, respectively. After molecular docking calculations, absorption, distribution, metabolism, and excretion/toxicity analysis was performed to examine the properties of various novel heterocyclic compounds for their future use as drugs.

GRAPHICAL ABSTRACT

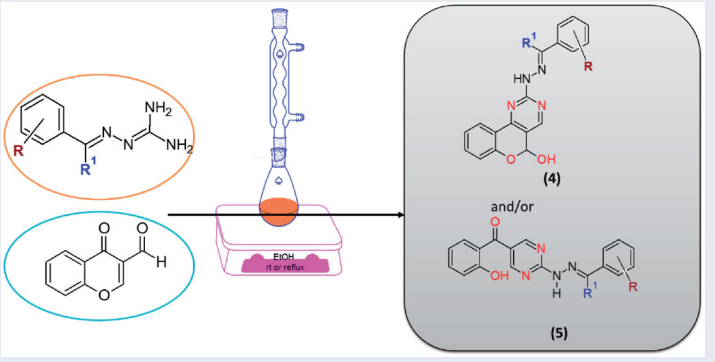

ARTICLE HISTORY

Received 28 February 2021

KEYWORDS

Antiproliferative activity; HepG2; MDA-MB-231; pyrimidine; molecular docking

CONTACT Emin Saripinar emin@erciyes.edu.tr Department of Chemistry, Faculty of Science, Erciyes University, Kayseri, Turkey.

Supplemental data for this article can be accessed on the publisher's website.

Introduction

Although newly introduced drugs today have significantly increased the success of treatment in many cancer types, nevertheless, there is still a need to develop more effective drugs for the treatment of breast, colon, liver, and many types of cancer. Heterocyclic compounds containing electron-rich nitrogen atoms are of great importance in this medicinal field.[1]

Synthetic drugs containing the pyrimidine nucleus, which is a structural component of critical drugs, are currently used in the clinics for treatments. These drugs have a very important role to play in many diseases.[2–5] Heterocyclic chemistry includes at least half of all organic chemistry research in the world. In particular, heterocyclic structures are the basis of many pharmaceutical, agricultural, and veterinary products forms. Heterocyclic compounds exhibit a high degree of structural diversity and wide therapeutic agents and play an effective role economically. Pyrimidine pharmacophore is an important and integral part of DNA and RNA[6] and plays an important role in biological processes.Due to its high activity, it has an outstanding recognition in organic and medicinal chemistry. Pyrimidine is the nucleus structural component[7] of critical drugs such as fluorouracil, etravirine, risperidone, iclaprim, avanafil, and rosuvastatin. Because of the wide range of biological activities of pyrimidines (anti-inflammatory, COX inhibitor, anticancer, antiallergic, analgesic, etc.) attention is drawn to the wide range broad class of compounds.[8] Because of their biological activities, they form an important group in the chemical compounds. Pyrimidine derivatives are known to be used in epilepsy,[9] measles disease treatments,[10] germs,[11] parasitic killers,[12] cancer chemotherapy,[13] and hepatitis B virus inhibitor.[14]

Chromones, heterocyclic compounds containing benzene ring condensed to the pyran ring is a large family of compounds, some of which are used as medicaments.

Chromones are an important class of natural and synthetic compounds with a broad spectrum of pharmacological activity such as anti-inflammatory, antibacterial, antitumor, anti-HIV, antioxidant, antiallergic, antiviral,[15–19] antifungal, antiulcer, immunostimulator, biological killer, wound curative, inflammation preventive, and antimicrobial.[20–33] 3-Formylchromone is a very active reagent and owing to the active centers in its structure, it has been reported to interact easily with the molecule. Chemical of substituted chromones reactivity depends on the nature and reaction conditions of the functional group present in the third position.

Among three-functionalized chromones, 3-formyl derivatives are widely used in heterocyclic synthesis. 3-Formylchromones provide a new pharmacophore for the treatment of diabetes (type II) and obesity as well as several tumor cells.[34] Biological activities could be as a result of the presence of an acting recipient of Michael α, β-unsaturated reactive aldehyde.[35–37]

3-Formylchromone (I) has three electrophilic centers. The first of these is carbonyl center C-4, the second is the formyl group in C, and the third is carbon with high reactive electrophilic properties of unsaturated C-2 carbon atoms.[38] In this case, the reaction of (I) with some reagents results in different yields leading to the formation of product mixtures.[39] As reported by Lowe, the reaction of 3-formylchromone with

formamidine, 5-(2-hydroxy benzoyl) pyrimidine (R = H, 13%) and 5-hydroxy-5H-chromeno[4,3-*d*]pyrimidine (R = H, 31%) mixtures were given with different C form substituted formamidine (R is alkyl, aryl, hetaryl, NH_2, NHCN, SH, SMe, OH, OMe, 1-pyrrolidinyl, or 1-piperidinyl, 4-morpholinyl) reaction with 26–90% yielded chromenopyrimidine.[40–42] Thus, 3-formylchromones can be used with 1,3-bifunctional nucleophiles which are amidine derivatives as a good precursor for the synthesis of pyrimidine derivatives. Based on the experiment of Bruno et al., Vilsmeier-Haack[43,44] started from the use of hydroxyacetophenone with ($POCl_3$ in DMF) to produce 3-formylchromone, 2-cycloamino-5-hydroxy-5H-[1]benzopyrano[4,3-*d*]pyrimidine intermediates to give pyrrolidine-1-carboxamidine hydrochloride, piperidine-1-carboxamidine sulfate or morpholine-4-carboxamidine hydrochloride (S-starting from methylisothioure sulfate and suitable amines) were used for the experiment. Subsequently, the hemiacetalic hydroxy at position 5 of the benzopyrano[4,3-*d*] pyrimidine system group was replaced with appropriate amines in the presence of $TiCl_4$.[42].

When many studies conducted in recent years are examined, the results of experimental and theoretical studies are seen together.[45–48] It has been observed that the work done in this way is of higher quality and realistic. Because it has been observed that the results obtained support each other, thus increasing the accuracy of the results. In these studies, it was observed that the numerical values of the results obtained from experimental and theoretical studies were quite close to each other. Therefore, when theoretical calculations are made before experimental studies, it has been seen that time will be an important guide for experimental studies. In this direction, it is possible to synthesize more effective and active molecules with theoretical calculations.

In theoretical calculations, molecular docking is the best method to compare the biological activities of molecules against enzymes.[49] In the calculations made by molecular docking method, theoretical biological activity values of molecules against enzymes are found. It is possible to compare the biological activities of other molecules with the numerical values obtained because of the calculation. Many parameters are obtained in calculations made new pyrimidine-chromeno hybrid derivatives against enzymes.

It provides important information about the biological activities of molecules with the parameters obtained because of these calculations. After these calculations, new pyrimidine-chromeno hybrid derivatives absorption, distribution, metabolism, excretion /Toxicity(ADME/T) analysis was performed.[50–53] With the ADME/T analysis, the effects and reactions of drug molecules in human metabolism in cells and tissues are tried to be predicted theoretically. These effects and responses are tried to be predicted by numerical values of parameters found by ADME/T calculations in molecular docking calculations. The numerical value of each parameter obtained gives important information about the action and reaction of molecules in different organs or tissues. These results give the properties of the molecule to be used as a drug in the future.

Guanylhydrazones known as amidinohydrazones, with oxo compounds (aldehyde/ketone), were obtained from the reaction of aminoguanidine. These compounds are antiprotozoal, antibacterial, antimalarial, tripanosidal, antisecretory, antidiuretic, anticoagulant, antihypertensive, antiviral, and possess anticancer activities. Other than medical importance, it could also be used for the synthesis of important heterocyclic compounds. The importance of both 3-formylchromone and guanylhydrazones was also considered in our reactions. In a

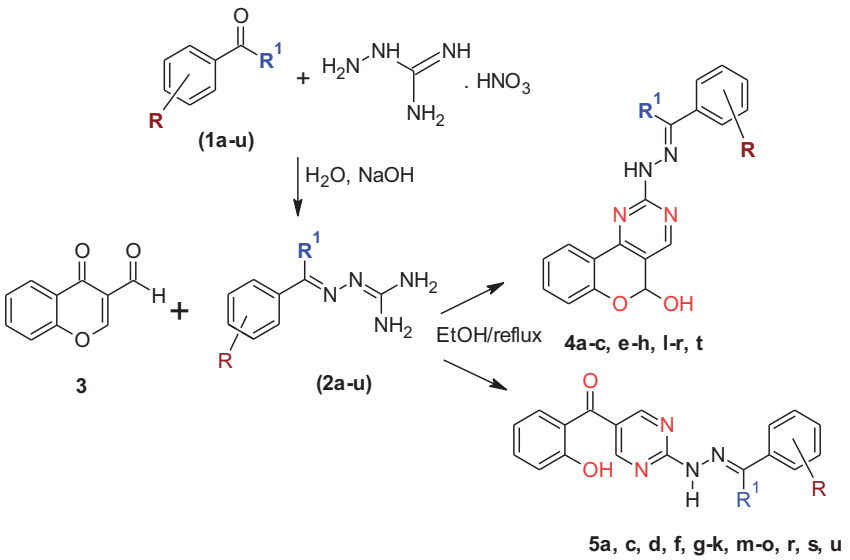

Scheme 1. A synthesis scheme of compound 5*H*-chromeno[4,3, *d*]pyrimidine (**4a–c**, **e–h**, **1–r**, **t**) and pyrimidine-5-yl-(2-hydroxyphenyl)methanone (**5a**, **c**, **d**, **f**, **g–k**, **m–o**, **r**, **s**, **u**) derivatives.

literature review, some pyrimidine-chromeno hybrid heterocyclic compounds containing nuclei have been shown to exhibit biological activity. Due to the active centers in the 3-formylchromone structure, it is known that the reactivity against nucleophilic substances is quite high and it interacts easily with many molecules. These compounds are versatile substrates that can be used as raw materials for synthetic drug synthesis. Due to above mentioned properties of these compounds, new molecules having pyrimidine-chromeno structure were synthesized and characterized. The antiproliferative activities of these synthesized compounds were studied as *in vitro*.

Results and discussion

Although numerous pyrimidine-chromeno compound derivatives have been introduced to the literature up to today, there is still a need to synthesize novel compound derivatives containing the pyrimidine nucleus in view of the broad biological properties of these compounds.

In many structure-activity studies, it has been found that substitution with donor/electron-withdrawing groups on aryl rings or binding of aryl/heteroaryl groups to the functional structure has a significant effect on anticancer activity. Designed molecules were synthesized, as shown in Scheme 1.

Pyrimidine-5-yl-(2-hydroxyphenyl)methanone and 5*H*-chromeno[4,3-*d*]pyrimidine-derived compounds were synthesized. A product mixture was obtained from the reaction of **3** and **2a-u** derivatives. Because of compound **3** having three electrophilic centers, it mainly produces two products after synthesis. This may result in different yields in a reaction when mixed with different reagents. When the reaction scheme is examined, it will be seen that **3** and **2a–u** reaction will result in the formation of a product

Table 1. Some characteristic data and properties of synthesized compounds.

Entry	Compound	R	R^1	Melting point (°C)	^{1}H NMR$_{(OH)}$ (δ, ppm)	IR$_{(C=O)}$ (cm^{-1})	Color	Yield (%)
1	**4a**	4-CH_3	H	251–253	11.37		Yellow	11
2	**5a**	4-CH_3	H	213–215	11.89	1600.8	Yellow	82
3	**4b**	H	H	256–258	11.45		Cream	70
4	**4c**	2-Cl	H	260–262	11.70		Yellow	68
5	**5c**	2-Cl	H	221–223	12.15	1590.9	Yellow	26
6	**5d**	4-CH_3O	H	243–245	11.84	1594.3	Yellow	71
7	**4e**	H	CH_3	217–218	10.27		Yellow	85
8	**4f**	4-NO_2	H	269–271	11.83		Yellow	14
9	**5f**	4-NO_2	H	260–262	11.27	1614.2	Yellow	70
10	**4g**	4-Cl	H	243–245	11.56		Cream	21
11	**5g**	4-Cl	H	208–210	12.01	1615.0	Yellow	65
12	**4h**	4-N$(CH_3)_2$	H	221–223	11.11		Yellow	12
13	**5h**	4-N$(CH_3)_2$	H	231–233	11.67	1655.2	Yellow	80
14	**5i**	4-CH$(CH_3)_2$	H	209–211	11.90	1582.6	Yellow	83
15	**5j**	4-CH_3CH_2O	H	168–170	11.81	1597.5	Yellow	91
16	**5k**	2-Cl-6-F	H	233–234	12.12	1574.3	Yellow	69
17	**4l**	4-CH_3O	CH_3	234–245	10.14		Yellow	94
18	**4m**	2,4-*di*CH_3O	H	198–201	11.25		Yellow	13
19	**5m**	2,4-*di*CH_3O	H	212–213	11.77	1599.7	Yellow	82
20	**4n**	4-CF_3	H	238–240	11.67		Yellow	13
21	**5n**	4-CF_3	H	245–247	12.14	1579.6	Yellow	67
22	**4o**	4-Cl	CH_3	233–235	11.33		Yellow	10
23	**5o**	4-Cl	CH_3	219–221	10.98	1600.8	Yellow	78
24	**4p**	2,6-*di*F	H	226–228	11.61		Yellow	72
25	**4r**	2,4-*di*Cl	H	249–251	11.78		Yellow	66
26	**5r**	2,4-*di*Cl	H	235–237	12.06	1599.6	Yellow	13
27	**5s**	4-F	H	184–186	12.01	1602.0	Cream	77
28	**4t**	3,4-*di*CH_3O	H	185–187	11.26		Yellow	59
29	**5u**	3-Br	H	225–227	11.99	1568.1	Yellow	73

or product mixture. In this type of experiment, normally two types of products are formed. But in some syntheses, only one product is formed, and second products are not formed or could not be fully purified. The resulting products have been represented in the form of "**4**" and "**5**". They were represented as **4** and **5** because of the change in the original skeletal structure of the compound. Products marked with "**4**" refers to pyrimidine compound derivatives 5*H*-chromeno[4,3,*d*], while products designated with "**5**" refers to compound derivatives of pyrimidine-5-yl-(2-hydroxyphenyl)methanone. **4a–c**, **e–h**, **l–r**, **t** and **5a**, **c**, **d**, **f**, **g–k**, **m–o**, **r**, **s**, **u** was obtained in yields of 11¯94%. All spectral data, with the structure of compounds **4a–c**, **e–h**, **l–r**, **t** and **5a**, **c**, **d**, **f**, **g–k**, **m–o**, **r**, **s**, **u** is consistent. Selected properties of compounds **4a–c**, **e–h**, **l–r**, **t** and **5a**, **c**, **d**, **f**, **g–k**, **m–o**, **r**, **s**, **u** is given in Table 1.

Compounds represented by "**4**" contain chromene, while compounds represented by "**5**" contain C=O. Thus, the ^{1}H NMR and ^{13}C NMR spectra of the synthesized compounds show different chemical shift values. The exception of alkyl groups demonstrated similar structures and characteristic signals that are common. As shown in Scheme 1, guanylhydrazone derivatives (**2a–u**) obtained by reaction of oxo compounds (aldehyde/ketone; **1a–u**) with aminoguanidine reacted with **3**. The diversity in the series results from the presence of electron donor-withdrawing groups of substituents attached to aromatic rings present in **1a–u**. In general, the yields were satisfactory. A substituent electron donor group attached to the ring was observed to be more efficient in reactions. First, the reaction product obtained as a single

product and that of two different products **4l** and **5d** base on the structure of the compounds is explained in detail based on spectroscopic data. After obtaining a single crystal of **4l** and **5d** compounds after the synthesis, X-ray single-crystal studies were also carried out.

When the Fourier transform- infrared (FT-IR) spectrum of compound **4l** was examined, NH, C–H, C=N, and C–O groups with typical frequency values of 3305.3, 3053.4–2842.5, 1602.8–1581.2, and 1551.8–1510.5 cm^{-1} were observed. When the ^1H NMR spectra of compound **4I** were examined, whereas the proton of the O*H* group located on the fifth position carbon of the chromeno ring showed a characteristic singlet signal of $\delta = 10.14$ ppm, the signal of *H* which is bound to the same position on the carbon showed $\delta = 6.46–6.47$ ppm due to geminal interaction of protons which showed a doublet signal. This peak was seen specifically in the compound derivatives represented by "**4**". The proton on the -NH group showed a signal of $\delta = 7.61$ ppm. In the presence of –OH and –NH protons after the addition of deuterium oxide (D_2O), the intensity of the peaks of their protons was seen to decrease or disappear because of displacement with deuterium. When the displacement of ^1H NMR D_2O spectrum was observed, the peaks of the protons of OH and NH of **4b** and **4e** (δ_{4b}: 11.45 and 7.63 ppm; δ_{4e}: 10.27 and 7.63 ppm) were seen to disappear (in Figure S8 and Figure S22). Protons bound to carbons in the aromatic ring (Ar-H), showed a signal between δ: 8.51–6.98 ppm. Singlet peaks of CH_3O– and –CH_3 protons are obtained at $\delta = 3.80$ ppm and $\delta = 2.39$ ppm, respectively. When the ^{13}C NMR spectrum of compound **4l** was examined, the carbon (OCHOHC) on the fifth position of the chromene ring was seen to have a signal of $\delta = 91.27$ ppm by giving a characteristic signal of the structure illumination. The presence of carbon atoms (Ar-C) in the aromatic region was seen with signals δ: 161.36–114.13 ppm. The peaks of the CH_3O– and –CH_3 carbons are obtained at $\delta = 55.64$ ppm and $\delta = 14.04$ ppm, respectively.

When the FT-IR spectrum of compound **5d** was examined, NH, C-H, C=O, and the C=N groups were observed at 3227.8, 3111.7–2972.7, 1594.3, and 1532.6–1512.6 cm^{-1}. It was observed that the frequency displayed absorption bands showing vibration peaks confirming the structure of the substance. When the ^1H NMR spectra of the compound **5d** were examined, the –OH group bound to the aromatic ring showed a characteristic singlet signal at $\delta = 11.84$ ppm, while the –NH nitrogen-dependent proton showed the spectrum of the group at a characteristic singlet signal at $\delta = 10.43$ ppm. Equivalent protons bound to carbons in the pyrimidine ring (NCHCCHNC) showed $\delta = 8.70$ ppm at very close chemical shift values as a singlet signal. The proton of the imine (CCHNNHC) group showed a characteristic sharp singlet peak around 8.19 ppm. The protons bonded to carbons in the aromatic ring (Ar-H) were signaled in the range of 6.94–7.66 ppm. The methoxy (CH_3O-) group connected to the aromatic ring showed a singlet peak at 3.79 ppm.

When the ^1H NMR D_2O change spectrum was examined, −OH and −NH proton peaks (δ_{5d}: 11.84 and 10.43 ppm) after the addition of D_2O proton it was observed that the intensity of the peaks decreased because of displacement with deuterium (Fig. S18). Thus, the chemical shift value of –OH and –NH proton peaks were clarified. When the ^{13}C NMR spectra of compound **5d** were examined, the guanylhydrazone derivative of compound **3**, C = O group, formed by ring-opening during the

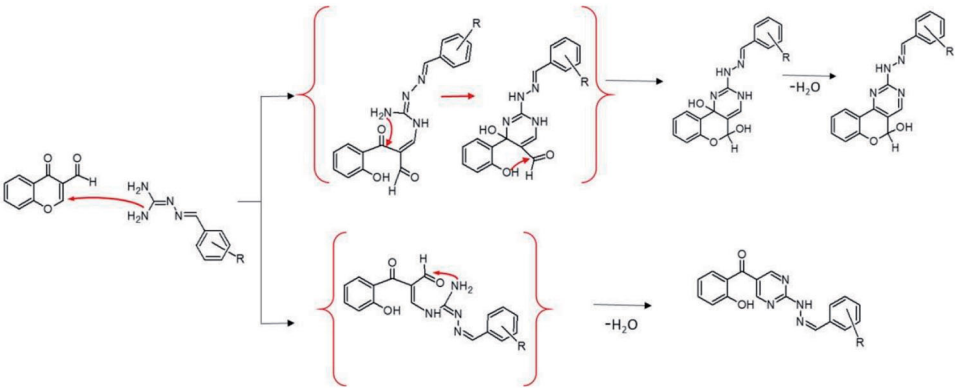

Scheme 2. Possible reaction mechanism.

reaction was observed to be δ = 192.87 ppm. The carbon groups present in the pyrimidine ring derived from the guanylhydrazone derivative imine (CCHNNHC) and the presence of carbon atoms (Ar-C) in the aromatic region, showed peaks between δ = 161.02 and 114.78 ppm. The signal of the carbon in the CH_3O- group was observed at δ = 55.73 ppm.

In the literature, while the proton at the fifth position of the benzopyran[4,3-*d*] pyrimidine system gives a peak between δ= 6.39 and 6.55 ppm, the chemical shift value was observed to be between δ= 6.43 and 6.51 ppm. While the signal of the fourth position proton on the structure was showing 8.10–8.55 ppm from experimental results however the signal observed was between δ = 8.26 and 8.55 ppm. Characterization data were found to be in harmony with the product symbolized as "**4**" in our study. Likewise, the characteristic spectra of 5-(2-hydroxybenzoyl)pyrimidine derivatives, which are represented as **5** are consistent with the data in the literature.[40]

3-Formylchromone, which has three electrophilic centers, particularly high electrophilic unsaturated C-2 carbon atom opens the ring by attacking the nucleophilic guanylhydrazone amine groups. The known Michael addition reaction mechanism observed on the α,β-unsaturated carbonyl compounds resulting in the splitting of the ring can be carried out in two ways. This condition, however, has led to the formation of product mixtures. The possible reaction mechanism is given in Scheme 2.

Cytotoxic activity studies

The synthesized compounds containing pyrimidine-chromeno nucleus were tested toward two different cancer cell lines using MTT assay method. The results obtained are given in Table 2.

Two series of heterocyclic organic compounds were tested against human breast adenocarcinoma cell line (MDA-MB-231) and human liver hepatocellular carcinoma cell line (HepG2) cell lines at concentrations ranging from 5–200 µM for 48 h. The structure-activity relationship (SAR) studies of the 5*H*-chromeno[4,3-*d*]pyrimidin-5-ol (**4**) and pyrimidine-5-yl-(2-hydroxyphenyl)methanone (**5**) demonstrate that cytotoxic activities of these compounds are mostly dependent on the position of R group, which

Table 2. IC_{50} results of compounds against MDA-MB-231and HepG2 cells.

	IC_{50} (μM)	
Compounds	MDA-MB-231	HepG2
4a	>200	48.61
5a	>200	95.59
4b	>200	66.38
4c	65.21	67.03
5c	>200	>200
5d	88.54	103.40
4e	119.30	99.59
4f	>200	>200
5f	>200	>200
4g	>200	71.22
5g	155.20	199.90
4h	152.00	51.99
5h	198.00	51.56
5i	96.66	80.88
5j	163.80	35.87
5k	>200	154.70
4l	>200	53.27
4m	N.T.	13.56
5m	>200	82.37
4n	>200	97.67
5n	199.40	44.23
4o	>200	65.68
5o	N.T.	194.80
4p	>200	>200
4r	>200	146.90
5r	>200	22.76
5s	186.55	83.30
4t	>200	70.88
5u	>200	183.30
Cisplatin	2.78	31.68
Melphalen	25.88	187.70
Ploxal-S	4.30	22.25
Fluorouracil	N.T.	146.90

N.T.: Not tested.

is dependent on the benzylidenehydrazin, namely: –F, –Cl, –Br, $–CH_3$, $–CF_3$, $–OCH_3$, $–CH(CH_3)_2$, $–OCH_2CH_3$, $–NO_2$, or $–N(CH_3)_2$. For instance, the most potent anticancer drug candidate **4c** against the MDA-MB-231 cell line has –Cl group on meta position of benzylidene ring. Compounds **4a**, **5a**, **4b**, **5c**, **5f**, **4 g**, **5h**, **5k**, **4l**, **5 m**, **4n**, **5n**, **4o**, **4p**, **4r**, **5r**, **4t**, and **5u** were found not to have cytotoxic activity toward breast cancer cell line. On the other hand, compound **4f** having an electron-withdrawing group ($–NO_2$), located in the para position of benzylidene ring, was also seen not to have cytotoxic activity in the same cell line. Compounds **4c**, **5d**, and **5i** were more potent than other compounds in MDA-MB-231 cell line, with the half maximal inhibitory concentration (IC_{50}) values 65.21, 88.54, and 96.66 μM, respectively.

The effects of all compounds were also screened in the HepG2 cell line. Compounds, except **5c**, **4f**, **5f**, **5 g**, **5o**, and **4p**, exhibited antiproliferative activities against HepG2 cell line. Compounds **5n**, **5j**, **4a**, and **5r** were especially found to be more effective potential anticancer drug candidates than the commonly used positive control drugs cisplatin, melphalen, and fluorouracil in HepG2 cells as they showed IC_{50} values of 44.23, 35.87, 48.61, and 22.76 μM, respectively. Furthermore, compound **4m** showed better antiproliferative activities than ploxal-S and other positive control drugs with following IC_{50}

value of 13.56 μM in HepG2. This is a remarkable result indicating that compound **4m** may be a possible drug candidate for liver cancer.

As shown in Table 2, compounds **5c**, **4f**, **5f**, and **4p** displayed a similar trend with IC_{50} values greater than 200 μM toward both HepG2 and MDA-MB-231. It is noteworthy that although compounds **4a**, **4b**, **4c**, **4g**, **4h**, **5h**, **5j**, **4 l**, **4m**, **5n**, **4o**, **5r**, and **4t** showed measurable antiproliferative activities in HepG2, it was found to have no cytotoxic activity in MDA-MB-231. Therefore, these compounds have more suitability for further research on liver cancer rather than on breast cancer.

Such as the substituent depending on designed compounds, the drug concentration of compounds has a significant role on screened cell lines. The live-cell percentages were observed to increase with decreasing concentrations of tested heterocyclic organic compounds toward MDA-MB-231 and HepG2 (Figs. S91 and S92). The most cell viability ratio was obtained at 5 μM of tested compounds in HepG2 and MDA-MB-231.

Molecular docking studies

As a result of molecular docking calculations, many parameters of new pyrimidine-chromeno hybrid derivatives against enzymes were found. These parameters are given in the Table 3. As a result of the calculations, the most important parameter among the parameters found is the docking score. It should be well known that the molecule with the most negative numerical value of the docking score parameter obtained because of the interaction between molecules and enzymes has higher biological activity than other molecules.[54] As the interaction between new pyrimidine-chromeno hybrid derivatives and enzyme increases, the biological activity value of new pyrimidine-chromeno hybrid derivatives increases, showing both experimental and theoretical results.

After the docking calculations made to compare the biological activities of molecules, the drug-ability properties of new pyrimidine-chromeno hybrid derivatives were examined. As a result of the ADME/T analysis, many parameters were found for the molecule. These calculated parameters give the effects and responses of new pyrimidine-chromeno hybrid derivatives in human metabolism of tissues or organs.[55] As a result of this analysis, each parameter is numerical value in different organs or tissues. All the calculated parameters are detailed in Table 4. Molecules marked with "–" in Table 4 did not show any interaction with cancer proteins.

Many other parameters were found in the calculations. These parameters are used to explain the interaction between the new pyrimidine-chromeno hybrid derivatives and the enzyme. Other parameters found because of the calculations are Glide hbond, Glide evdw, and Glide ecoul parameters. These parameters give numerical values of hydrogen bonding, Van der Waals, and Coulomb interactions, which are many interactions between molecules and enzymes. These interactions have many interactions such as hydrogen bonds, polar and hydrophobic interactions, π-π and halogen.[56] These are given in Figures 1–6. On the other hand, the last remaining parameters are Glide emodel, Glide energy, Glide einternal, and Glide posenum parameters, which gives numerical value about the interaction exposure between new pyrimidine-chromeno hybrid derivatives and enzyme.[57]

Table 3. Numerical values of the parameters obtained from interaction of studied molecule with cancer cells.

Breast cancer	Docking score	Glide ligand efficiency	Glide hbond	Glide evdw	Glide ecoul	Glide emodel	Glide energy	Glide einternal	Glide posenum
4a	−3.53	−0.14	−0.41	−26.91	−3.93	−37.21	−30.85	0.45	117
4b	−3.52	−0.15	−0.33	−27.50	−3.44	−37.71	−30.94	0.07	378
4c	−3.56	−0.14	−0.34	−28.53	−3.55	−39.24	−32.08	0.06	331
4e	−3.70	−0.15	−0.36	−27.39	−3.94	−38.40	−31.33	0.09	265
4f	−3.90	−0.14	−0.31	−31.45	−5.02	−44.71	−36.47	1.17	304
4g	−4.45	−0.14	−0.06	−30.31	−3.12	−39.73	−33.44	1.33	245
4h	−3.25	−0.12	−0.33	−29.52	−3.06	−39.10	−32.57	0.20	338
4l	−3.51	−0.13	−0.44	−29.05	−3.75	−36.92	−32.80	5.25	256
4m	−3.50	−0.12	−0.18	−29.40	−4.44	−39.44	−33.83	3.86	342
4n	–	–	–	–	–	–	–	–	–
4o	–	–	–	–	–	–	–	–	–
4p	–	–	–	–	–	–	–	–	–
4r	–	–	–	–	–	–	–	–	–
4t	−4.45	−0.16	−0.63	−22.51	−11.01	−42.68	−33.52	5.58	330
5a	−2.99	−0.12	0.00	−25.05	−3.45	−38.56	−28.50	0.14	5
5c	−2.67	−0.11	−0.16	−21.52	−4.16	−25.81	−25.68	9.34	12
5d	−3.73	−0.14	−0.42	−26.70	−5.92	−36.04	−32.62	19.63	308
5f	–	–	–	–	–	–	–	–	–
5g	−3.54	−0.14	−0.32	−23.33	−3.65	−37.79	−26.98	0.29	265
5h	−2.58	−0.10	0.00	−27.85	−0.28	−38.53	−28.13	0.64	316
5i	−2.72	−0.10	−0.25	−17.50	−4.65	−31.48	−22.15	1.00	265
5j	−2.79	−0.10	−0.05	−24.09	−4.39	−35.63	−28.48	6.47	225
5k	−2.75	−0.11	0.00	−25.10	−2.20	−35.41	−27.30	4.40	296
5m	−1.75	−0.06	−0.13	−25.80	−2.70	−29.55	−28.51	5.87	323
5n	−2.10	−0.08	0.00	−16.47	−2.57	−25.53	−19.04	1.52	319
5o	−3.43	−0.14	−0.32	−24.08	−2.60	−37.33	−26.69	0.29	265
5r	−2.91	−0.11	−0.16	−21.23	−3.53	−32.03	−24.76	3.97	202
5s	−2.62	−0.10	0.00	−23.68	−0.84	−33.42	−24.51	1.21	264
5u	−2.19	−0.09	0.00	−25.56	−0.80	−34.44	−26.35	1.85	153
Liver cancer	Docking Score	Glide ligand efficiency	Glide hbond	Glide evdw	Glide ecoul	Glide emodel	Glide energy	Glide einternal	Glide posenum
4a	−7.61	−0.30	−0.11	−38.43	−2.81	−56.68	−41.24	8.47	146
4b	−7.38	−0.31	0.00	−41.49	−2.92	−60.41	−44.42	5.51	102
4c	−5.63	−0.23	0.00	−35.63	−1.43	−50.33	−37.06	0.17	295
4e	−6.47	−0.26	0.00	−32.94	−1.65	−45.06	−34.59	3.14	102
4f	−6.31	−0.25	0.00	−33.04	−1.30	−46.60	−34.34	1.67	166
4g	−7.84	−0.29	−0.11	−43.55	−3.56	−63.90	−47.11	9.22	175
4h	−8.40	−0.34	−0.13	−40.73	−4.40	−60.06	−45.12	13.34	201
4l	−8.08	−0.30	−0.11	−41.65	−2.71	−59.91	−44.36	9.60	175
4m	−6.23	−0.23	0.00	−39.53	−2.10	−55.49	−41.63	1.53	135
4n	−8.62	−0.20	−0.27	−35.84	−1.69	−47.42	−37.53	4.20	22
4o	−7.28	−0.26	0.00	−38.59	−2.28	−57.40	−40.87	1.76	169
4p	−8.45	−0.33	−0.16	−41.69	−5.04	−55.82	−46.73	21.89	66

4r	−7.49	−0.29	0.00	−40.16	−1.98	−55.38	−42.14	8.80	203
4t	−6.66	−0.26	0.00	−40.17	−0.53	−48.36	−40.70	13.49	72
5a	–	–	–	–	–	–	–	–	–
5c	–	–	–	–	–	–	–	–	–
5d	–	–	–	–	–	–	–	–	–
5f	–	–	–	–	–	–	–	–	–
5g	–	–	–	–	–	–	–	–	–
5h	−7.73	−0.29	0.00	−34.06	−1.08	−31.81	−35.15	23.97	278
5i	−7.74	−0.29	−0.16	−29.87	−3.78	−55.41	−33.66	4.34	157
5j	−7.82	−0.29	0.00	−36.22	−1.37	−41.92	−37.59	21.66	311
5k	−6.26	−0.24	0.00	−10.22	−3.65	−8.52	−13.86	29.28	124
5m	−6.58	−0.24	0.00	−28.97	0.60	−30.14	−28.37	23.47	133
5n	−8.38	−0.30	−0.23	−31.50	−4.87	−51.99	−36.37	11.16	70
5o	−7.82	−0.31	0.00	−32.46	−1.25	−40.11	−33.71	20.89	400
5r	−7.05	−0.27	−0.24	−39.22	−3.01	−45.69	−42.23	31.21	262
5s	−6.92	−0.28	−0.16	−32.76	−1.96	−35.27	−34.72	26.28	356
5u	−7.88	−0.32	−0.21	−41.45	−1.28	−58.04	−42.73	10.01	64
Lung cancer	Docking Score	Glide ligand efficiency	Glide hbond	Glide evdw	Glide ecoul	Glide emodel	Glide energy	Glide einternal	Glide posenum
4a	−5.36	−0.21	0.00	−34.16	−1.86	−47.45	−36.02	1.96	8
4b	−5.58	−0.23	−0.02	−29.54	−4.82	−45.25	−34.36	2.15	81
4c	−5.01	−0.20	−0.08	−24.86	−8.83	−44.51	−33.69	0.31	213
4e	−5.61	−0.22	−0.04	−32.96	−5.13	−52.65	−38.10	0.58	271
4f	−6.19	−0.23	0.00	−33.16	−6.03	−46.30	−39.20	11.16	133
4g	−8.92	−0.36	−0.32	−35.01	−3.24	−57.14	−38.25	4.55	158
4h	−5.31	−0.20	0.00	−31.06	−2.09	−41.94	−33.15	1.41	302
4l	−4.95	−0.18	−0.13	−25.72	−3.89	−38.31	−29.61	0.40	330
4m	−6.36	−0.23	−0.17	−30.91	−9.08	−51.55	−40.00	9.64	121
4n	–	–	–	–	–	–	–	–	–
4o	–	–	–	–	–	–	–	–	–
4p	–	–	–	–	–	–	–	–	–
4r	–	–	–	–	–	–	–	–	–
4t	−6.19	−0.22	−0.39	−27.63	−7.93	−47.10	−35.55	2.66	286
5a	–	–	–	–	–	–	–	–	–
5c	–	–	–	–	–	–	–	–	–
5d	–	–	–	–	–	–	–	–	–
5f	–	–	–	–	–	–	–	–	–
5g	–	–	–	–	–	–	–	–	–
5h	−6.93	−0.26	0.00	−43.26	0.81	−47.97	−42.44	11.19	231
5i	−4.95	−0.18	0.00	−21.87	−4.22	−23.29	−26.10	8.52	339
5j	−5.57	−0.21	0.00	−36.88	−1.78	−50.52	−38.67	10.16	389
5k	−5.35	−0.21	0.00	−37.53	−4.51	−58.27	−42.03	4.14	231
5m	−5.09	−0.18	0.00	−36.00	−4.91	−54.55	−40.91	7.35	289
5n	−5.43	−0.19	0.00	−24.19	−4.10	−38.13	−28.29	5.58	383
5o	−7.13	−0.29	0.00	−36.53	−0.46	−33.29	−37.00	28.15	265
5r	−9.64	−0.37	−0.31	−27.40	−9.19	−51.15	−36.58	7.36	8
5s	−7.87	−0.31	−0.28	−35.57	1.34	−24.21	−34.23	28.96	179
5u	−5.20	−0.21	0.00	−37.08	−4.31	−44.55	−41.39	14.54	246

The biological activities of the studied molecules against cancer proteins were compared. The molecules with the highest activity are **4t** and **4g** molecules against breast cancer protein, **4n** molecules against liver cancer protein, and **5r** molecules against lung cancer protein.

Among all ADME/T parameters, another important two parameters are Rule of five and Rule of three. The Rule of five[58,59] and Rule of three[60] parameters are more important than any other parameter. In the analysis for molecules, the numerical value of these two parameters is expected to be zero. The Rule of five parameter, also known as Lipinski's Pfizer's fifth rule. The rules are: mol MW <500, QPlogP o/w <5, donorHB ≤ 5, and accptHB ≤ 10. However, the Rule of three parameter is known as the three of Jorgensen's rule. The three rules are: QPlogS>-5.7, QP PCaco>22 nm / s, and #Primary Metabolites <7. If the numerical value of the Rule of three parameter is zero, this molecule can be used orally as a drug. These two parameters are the two parameters that best explain the drug properties of molecules.

X-ray diffraction analysis for 4l

The molecular structure of **4l**, with the atom numbering scheme, is shown in Figure 7. The N4 = C12 bond distance [1.282(5) Å] is a typical double bond character. The dihedral angles between pyrimidine and phenyl rings are 8.59(13) and 10.28(17)°. The dihedral angle of the phenyl rings is 6.54(18)°, respectively. The pyrimidine ring plane is approximately planar, with a maximum deviation from the least-squares plane being 0.0474(27) Å for atom C11. The values of the O1–C5/C9 ring puckering parameters: Q = 0.319 (2) Å, θ= 61.65(2)° and φ= 315 (2)°. The C14-C12 = N4–N3 angle is 178.6(3)°, respectively. The molecules of **4l** are connected by O–H···N hydrogen bonds. Atom O_2 acts as a hydrogen-bond donor, via atom H2A, to atom $N2^{i}$, forming a C(6) chain running which is parallel to the direction $[x+1/2, y, -z+1/2]$.

X-ray diffraction analysis for 5d

The molecular structure of **5d**, with the atom numbering scheme, is shown in Figure 8. The C7=O2 [1.234(5) Å] and N4=C12 [1.273(6) Å] bond distances are a typical double bond character. The C1–C7–C8 and C10–N3–N4=C12 angles are 122.0(4) and −172.8(4)°, respectively. The pyrimidine ring makes dihedral angles of 44.38(13) and 7.50(20)° with the two phenyl rings. The dihedral angle of the phenyl rings is 41.08(13)°, respectively. The pyrimidine ring plane is approximately planar, with a maximum deviation from the least-squares plane being 0.0292(24) Å for atom C10. The molecules of **5d** are connected by N–H···N and C–H···O hydrogen bonds. Atom N3 atom acts as a hydrogen-bond donor, via atom H3A, to atom $N1^{ii}$, forming a centrosymmetric $R_2^2(8)$ ring centered at (1, 1/2, 1). Similarly, atom C11 in the molecule at (x, y, and z) acts as a hydrogen-bond donor, via atom H11, to atom $O3^{i}$, forming a centrosymmetric $R_2^2(24)$ ring centered at (1/2, 1/2, 1/2). The combination of the hydrogen bonds generates a chain of edge fused $R_2^2(8)$ and $R_2^2(24)$ rings running parallel to the direction.

Table 4. ADME properties of molecules.

	4a	4b	4c	4e	4f	4g	4h	4l	4m	4n	4o	4p	4r	4t	Reference range
mol_MW	332	318	353	332	363	353	361	362	378	386	367	354	387	399	130–725
dipole (D)	1.2	0.9	2.1	1.5	7.0	2.4	1.7	3.2	3.5	3.4	2.6	1.9	2.0	3.2	1.0–12.5
SASA	638	606	621	630	647	630	675	660	668	658	655	618	646	547	300–1000
FOSA	136	49	49	102	49	49	192	191	223	50	102	48	49	455	0–750
FISA	106	106	101	94	208	106	114	94	103	106	94	103	101	92	7–330
PISA	396	451	413	434	390	404	369	375	342	385	387	389	366	0	0–450
WPSA	0.0	0.0	57.9	0.0	0.0	72.1	0.0	0.0	0.0	118.1	72.1	77.2	129.9	0.0	0–175
volume (A^3)	1085	1026	1063	1077	1104	1071	1168	1148	1168	1124	1122	1052	1108	1090	500–2000
donorHB	2	2	2	2	2	2	2	2	2	2	2	2	2	5	0–6
accptHB	7.0	7.0	7.0	6.5	8.0	7.0	8.0	7.2	8.4	7.0	6.5	7.0	7.0	11.8	2.0–20.0
glob (Sphere = 1)	0.8	0.8	0.8	0.8	0.8	0.8	0.8	0.8	0.8	0.8	0.8	0.8	0.8	0.9	0.75–0.95
QPpolrz (A^3)	37.8	36.0	37.1	37.9	37.9	37.4	40.3	39.5	39.3	39.3	39.2	36.5	38.5	33.0	13.0–70.0
QPlogPC16	12.3	12.1	12.5	12.4	13.1	12.7	12.9	12.6	12.7	11.8	13.0	11.4	13.1	10.5	4.0–18.0
QPlogPoct	19.1	18.6	19.2	18.9	20.7	19.3	20.5	19.8	20.4	20.3	19.7	19.0	19.9	24.2	8.0–35.0
QPlogPw	13.3	13.6	13.4	13.0	14.8	13.4	14.1	13.2	14.1	13.4	12.8	13.3	13.2	19.1	4.0–45.0
QPlogPo/w	2.8	2.5	3.0	3.1	1.8	3.0	2.8	3.1	2.7	3.5	3.6	2.9	3.4	−1.4	−2.0–6.5
QPlogS	−4.6	−4.1	−4.6	−4.6	−4.3	−4.8	−4.7	−4.7	−4.3	−5.4	−5.3	−4.6	−5.3	2.0	−6.5-0.5
CIQPlogS	−4.4	−4.1	−4.7	−4.5	−4.6	−4.7	−4.5	−4.8	−4.7	−5.4	−5.2	−4.8	−5.4	1.4	−6.5–0.5
QPlogHERG	−6.6	−6.7	−6.6	−6.7	−6.7	−6.6	−6.6	−6.5	−6.4	−6.7	−6.6	−6.5	−6.5	−5.5	*
QPPCaco (nm/sec)	989	989	1090	1261	104	989	823	1262	1036	988	1262	1046	1090	21	**
QPlogBB	−0.8	−0.8	−0.6	−0.7	−2.0	−0.7	−1.0	−0.8	−0.9	−0.6	−0.5	−0.6	−0.5	0.2	−3.0–1.2
QPPMDCK (nm/sec)	489	489	1127	635	43	1213	401	636	514	2165	1579	1374	2797	10	**
QPlogKp	−1.6	−1.4	−1.4	−1.3	−3.4	−1.6	−1.7	−1.4	−1.6	−1.6	−1.4	−1.6	−1.6	−6.7	Kp (cm/h)
IP (ev)	9.2	9.2	9.2	9.2	9.4	9.3	9.0	9.2	9.2	9.3	9.3	9.3	9.3	8.1	7.9–10.5
EA (eV)	0.8	0.8	0.8	0.7	2.3	0.8	0.8	0.8	0.7	0.9	0.8	0.8	0.8	−0.9	−0.9–1.7
#metab	2	1	1	2	2	1	2	3	3	1	2	1	1	0	1–8
QPlogKhsa	0.0	−0.1	−0.1	0.1	−0.2	0.0	0.0	0.1	−0.1	0.1	0.2	−0.1	0.1	−0.5	−1.5–1.5
Human oral absorption.	3	3	3	3	3	3	3	3	3	3	3	3	3	2	–
Per. human oral absorption	97	95	100	100	74	100	96	100	97	100	100	100	100	42	***
PSA	78	78	78	76	126	78	85	86	96	78	76	78	78	93	7–200
RuleOfFive	0	0	0	0	0	0	0	0	0	0	0	0	0	0	Maximum is 4
RuleOfThree	0	0	0	0	0	0	0	0	0	0	0	0	0	1	Maximum is 3
Jm	0.2	1.1	0.3	0.5	0.0	0.2	0.1	0.3	0.5	0.0	0.1	0.2	0.0	8.5	–

	5a	5c	5d	5f	5g	5h	5i	5j	5k	5m	5n	5o	5r	5s	5u	Reference range
mol_MW	332	353	348	377	353	361	360	362	371	378	386	353	387	336	397	130–725
dipole (D)	4.3	3.4	6.3	10.0	6.8	5.1	4.3	6.2	3.2	6.1	7.8	6.8	6.7	6.7	6.2	1.0–12.5
SASA	661	648	659	695	654	697	704	704	651	690	682	653	669	638	658	300–1000

(*continued*)

Table 4. Continued.

	5a	5c	5d	5f	5g	5h	5i	5j	5k	5m	5n	5o	5r	5s	5u	Reference range
FOSA	111	22	113	113	24	166	182	158	23	198	25	24	24	24	24	0–750
FISA	153	151	153	215	153	162	153	153	148	151	153	153	149	153	153	7–330
PISA	397	413	393	367	404	370	369	393	382	341	385	404	367	414	403	0–450
WPSA	0.0	62.1	0.0	0.0	72.1	0.0	0.0	0.0	97.6	0.0	118.2	72.1	129.9	46.8	77.5	0–175
volume (A^3)	1123	1103	1134	1192	1109	1205	1214	1206	1114	1204	1162	1108	1146	1079	1116	500–2000
DonorHB	1	1	1	1	1	1	1	1	1	1	1	1	1	1	1	0–6
AccptHB	6.3	6.3	7.0	8.3	6.3	7.3	6.3	7.0	6.3	7.8	6.3	6.3	6.3	6.3	6.3	2.0–20.0
glob (Sphere =1)	0.8	0.8	0.8	0.8	0.8	0.8	0.8	0.8	0.8	0.8	0.8	0.8	0.8	0.8	0.8	0.75–0.95
QPpolrz (A^3)	38.1	37.4	37.9	39.9	37.6	40.5	40.8	40.1	37.6	39.5	39.5	37.6	38.7	36.5	37.8	13.0–70.0
QPlogPC16	12.8	13.1	12.8	13.7	13.2	13.4	13.5	13.6	12.7	13.1	12.3	13.2	13.6	12.1	13.3	4.0–18.0
QPlogPoct	17.7	17.7	18.3	20.5	18.2	19.1	18.5	18.9	17.9	19.1	19.2	18.2	18.8	17.8	18.3	8.0–35.0
QPlogPw	11.1	11.2	11.6	13.2	11.2	11.9	10.8	11.5	11.0	11.8	11.1	11.2	11.0	11.2	11.2	4.0–45.0
QPlogPo/w	3.1	3.3	2.9	2.2	3.3	3.1	3.6	3.3	3.4	2.9	3.8	3.3	3.7	3.0	3.4	−2.0–6.5
QPlogS	−4.9	−4.9	−4.4	−4.5	−5.1	−5.0	−5.5	−5.0	−5.1	−4.5	−5.8	−5.1	−5.6	−4.7	−5.2	−6.5–0.5
CIQPlogS	−4.6	−5.0	−4.6	−4.7	−5.0	−4.8	−5.1	−4.9	−5.3	−4.9	−5.6	−5.0	−5.7	−4.6	−5.9	−6.5–0.5
QPlogHERG	−6.8	−6.8	−6.7	−6.8	−6.8	−6.8	−6.8	−7.0	−6.6	−6.5	−6.9	−6.8	−6.7	−6.8	−6.8	*
QPPCaco (nm/sec)	349	367	348	91	348	290	348	348	390	365	348	348	384	348	348	**
QPlogBB	−1.5	−1.3	−1.5	−2.3	−1.3	−1.7	−1.6	−1.7	−1.2	−1.6	−1.2	−1.3	−1.1	−1.4	−1.3	−3.0–1.2
QPPMDCK (nm/sec)	158	367	158	37	393	130	158	158	612	166	702	392	905	285	420	**
QPlogKp	−2.3	−2.2	−2.2	−3.4	−2.2	−2.4	−2.3	−2.1	−2.2	−2.2	−2.3	−2.3	−2.3	−2.2	−2.3	Kp (cm/h)
IP (ev)	9.4	9.5	9.5	9.7	9.4	8.9	9.4	9.5	9.5	9.4	9.7	9.4	9.5	9.6	9.5	7.9–10.5
EA (eV)	0.8	0.8	0.8	2.6	0.8	0.8	0.8	0.8	0.8	0.7	0.9	0.8	0.8	0.8	0.8	−0.9–1.7
#metab	4	3	4	4	3	4	4	4	3	5	3	3	3	3	3	1–8
QPlogKhsa	0.1	0.1	0.0	−0.1	0.1	0.1	0.3	0.1	0.1	0.0	0.2	0.1	0.2	0.0	0.1	−1.5–1.5
Human oral absorption	3	3	3	3	3	3	3	3	3	3	3	3	3	3	3	–
Per. human oral absorption	91	92	89	75	92	89	94	92	93	90	95	92	95	90	92	***
PSA	97	97	106	133	97	103	97	106	96	115	97	97	96	97	97	7–200
Rule of five	0	0	0	0	0	0	0	0	0	0	0	0	0	0	0	Maximum is 4
Rule of three	0	0	0	0	0	0	0	0	0	0	1	0	0	0	0	Maximum is 3
Jm	0.0	0.0	0.1	0.0	0.0	0.0	0.0	0.0	0.0	0.1	0.0	0.0	0.0	0.0	0.0	–

*Range below -5; **a < 25 is poor and a > 500 is great; ***b < 25 is poor and b > 80 is high.

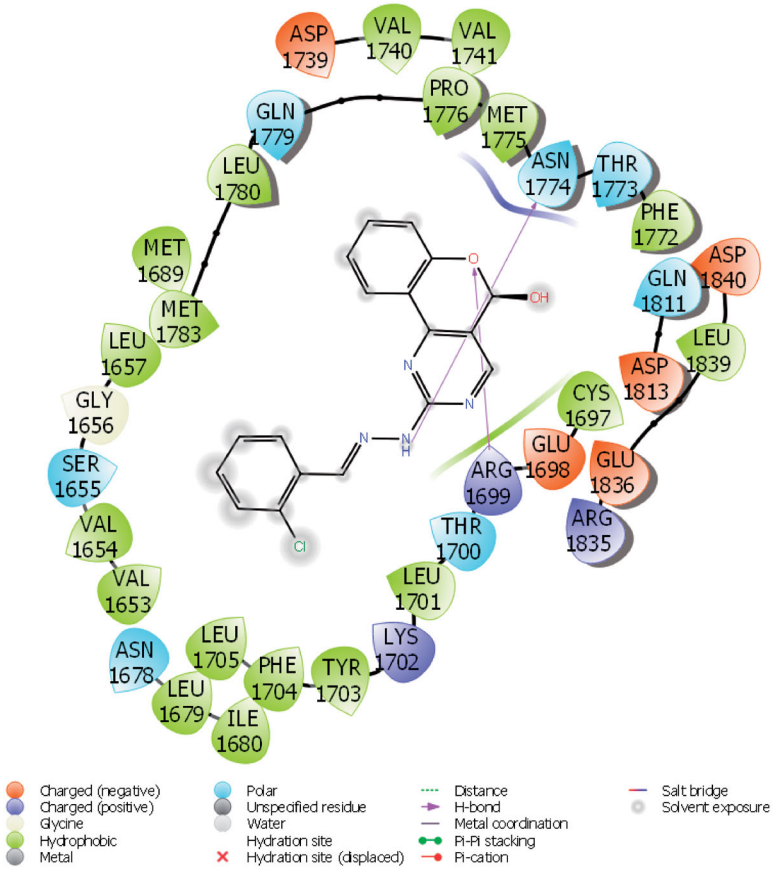

Figure 1. Representation of interactions between molecule **4c** and breast cancer protein.

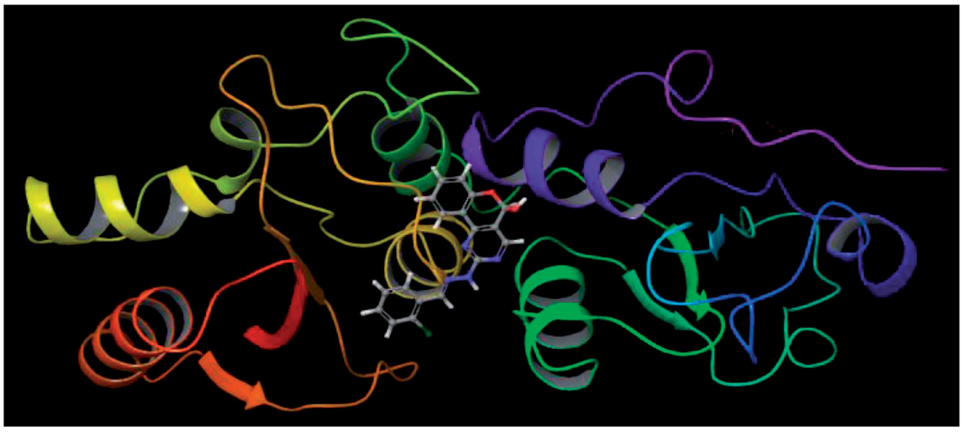

Figure 2. Representation of interactions between molecule **4c** and breast cancer protein.

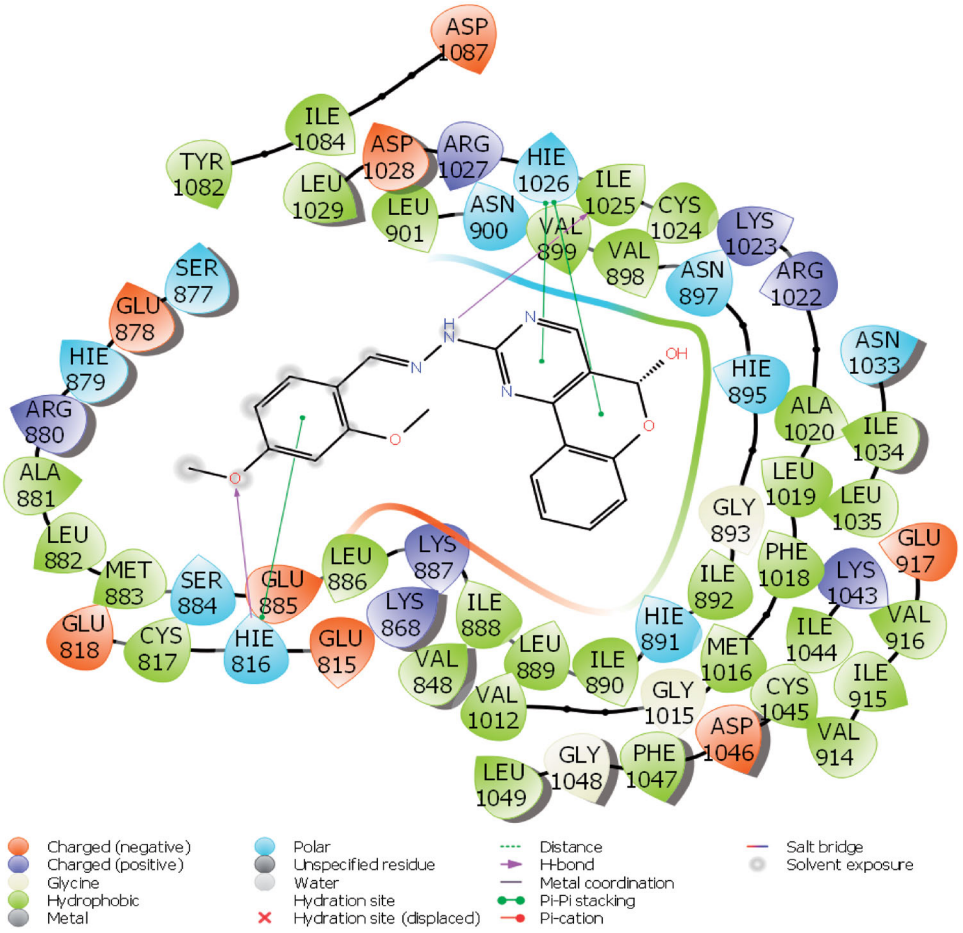

Figure 3. Representation of interactions between molecule **4m** and liver cancer protein.

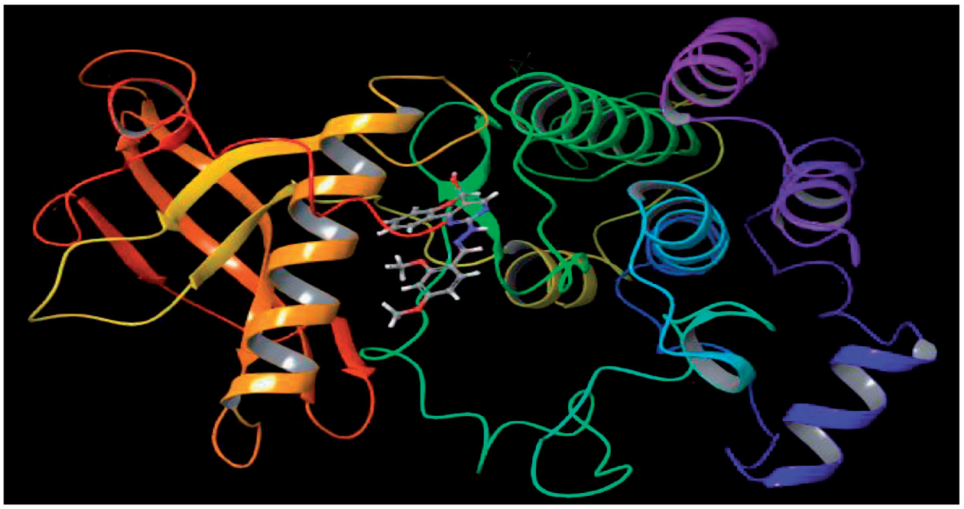

Figure 4. Representation of interactions between molecule **4m** and liver cancer protein.

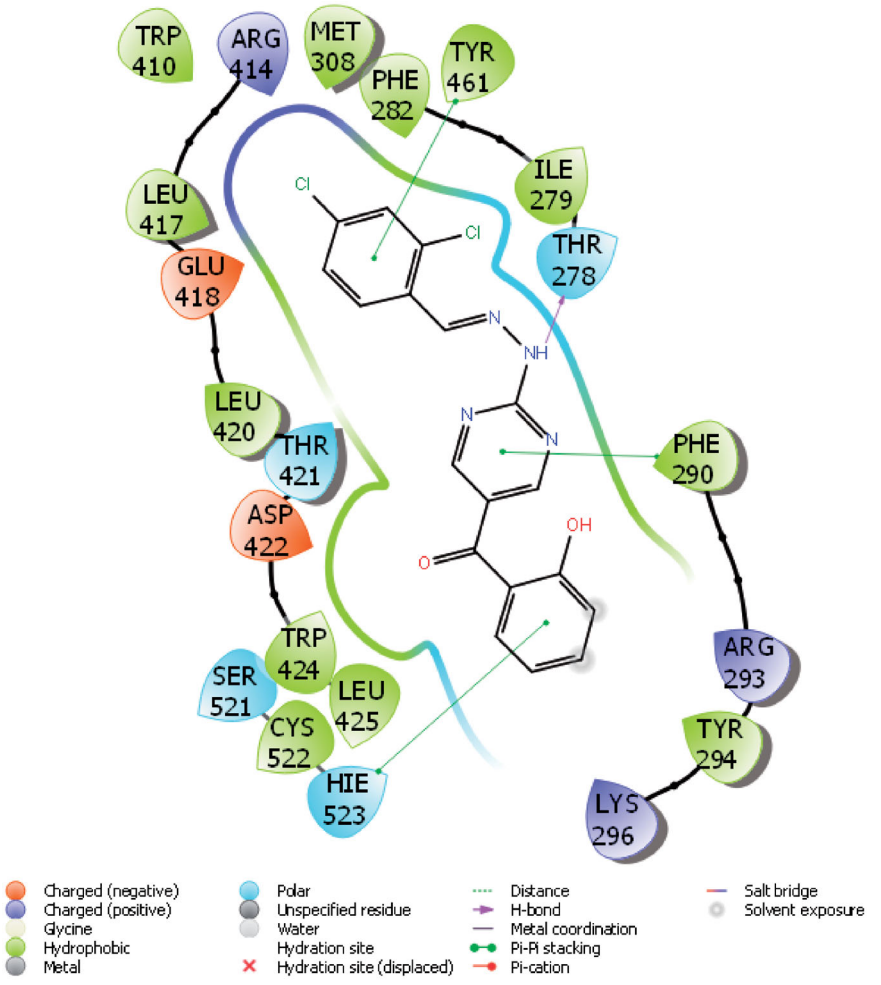

Figure 5. Representation of interactions between molecule **5r** and lung cancer protein.

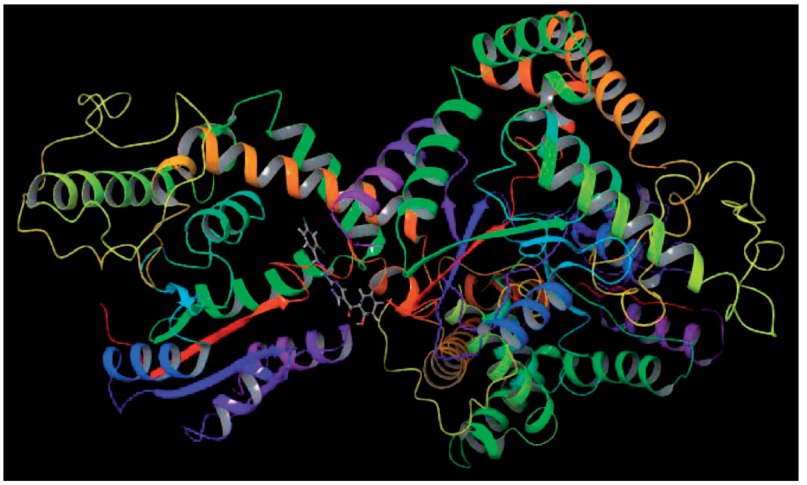

Figure 6. Representation of interactions between molecule **5r** and lung cancer protein.

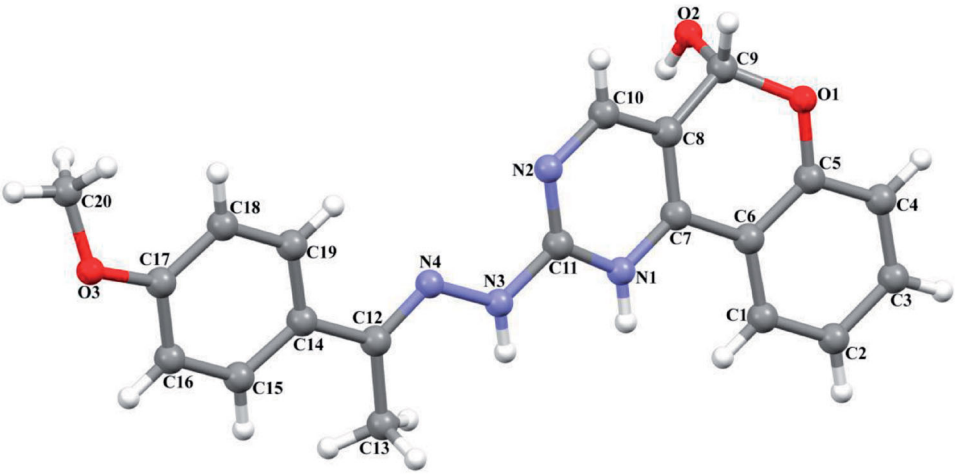

Figure 7. The molecular structure of **4l** showing the atom numbering scheme.

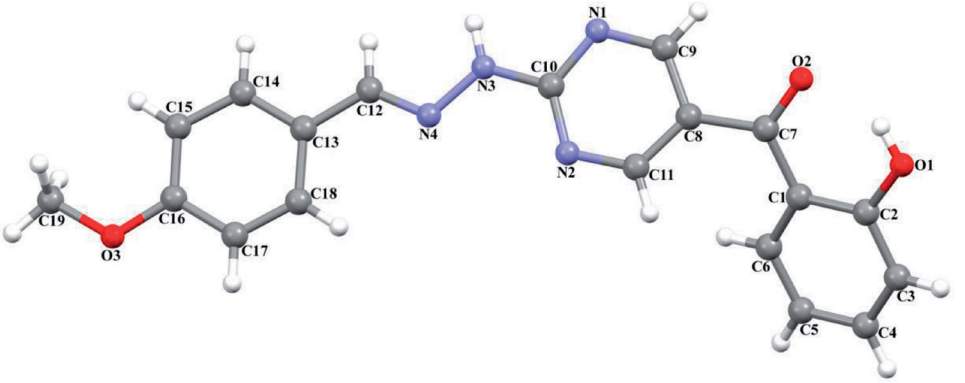

Figure 8. The molecular structure of **5d** showing the atom numbering scheme.

Conclusion

Novel 5*H*-chromeno[4,3-*d*]pyrimidine **(4a–c, e–h, l–r, t)** and pyrimidine-5-yl-(2-hydroxyphenyl)methanone **(5a, c, d, f–k, m–o, r, s, u)** derivatives were synthesized and characterized. Furthermore, the structures of compounds **4l** and **5d** were completely verified by X-ray crystal structural analysis. All compounds were screened against two human cancer cell lines using MTT assay. Most of the compounds were found to have more cytotoxic effects toward liver cancer cells than breast cancer cells. Particularly, compounds **4a**, **5a**, **4b**, **4g**, **4h**, **5h**, **5j**, **4l**, **5m**, **4n**, **5n**, **4o**, **5r**, **5s,** and **4t** exhibited anti-proliferative effects at lower micromolar concentrations in HepG2 cells rather than MDA-MB-231 cells. On the other hand, molecule **4m** exhibited the best activity with IC_{50} value of 13.56 µM against HepG2.

Biological activities of new pyrimidine-chromeno hybrid derivatives against enzymes were compared. As a result of these docking calculations, the molecules with the highest activity are **4t** and **4g** molecules against breast cancer protein, **4n** molecules against liver cancer protein, and **5r** molecules against lung cancer protein. The theoretical

calculations made are generally similar to the experimental results. However, the main reason for the differences occurred is that the theoretical calculations were made in a pure and isolated environment, but there are many experimental inputs in experimental processes. After examining the interaction of these new pyrimidine-chromeno hybrid derivatives against enzymes, a theoretical ADME/T analysis was made. Considering the interaction of the molecule with enzymes because of docking calculations, it is seen that it has a high interaction. Accordingly, since ADME/T parameters meet the necessary conditions, it is safe to use it as an advanced drug. The numerical values of the parameters obtained from this study are used in future *in vivo* and *in vitro* studies, providing a great deal for new drug candidate discovery.

Experimental section

For each of the series, parameters such as temperature, type of solvent, time, and catalyst were considered for the determination of the optimum reaction conditions of the experiment. During the synthesis, thin layer chromatography (TLC) application was used. With specific time intervals, the material from the reaction balloon and the starting reactant material are put in an already prepared solution with silica gel selected as adsorbent and the help of 60/F-254 coated aluminum applied to the plates with the aid of capillary tubes which aid dragging in moving phases. Reaction times were determined according to the TLC results. For each part of the experiment, TLC mobile phases were tested by using different solvent mixtures for the control of the synthesis. The impurity controls were first performed by TLC and the compounds that contained impurity were purified by washing, crystallization, and purification by column chromatography. 9200 melting point apparatus was used to define the melting points (m.p.) of each of the compounds. The structures of the products obtained were confirmed by using nuclear magnetic resonance (NMR, ^{1}H and ^{13}C NMR), FT-IR, elemental analysis, and X-ray diffraction.

A general method for the synthesis of compounds 5H-chromeno[4,3-d]pyrimidine (4a) and pyrimidine-5-yl-(2-hydroxyphenyl) methanone (5) derivatives

Guanylhydrazone derivatives (**2a**-**u**; 1 mmol) and 3-formylchromone (**3**; 1 mmol) were added to a 100 ml flask. The mixture was stirred under reflux for 3–8 hours in 10 cm^3 of ethyl alcohol. The precipitates were filtered, and the impurity was checked by TLC. In column chromatography (**4a**, **c**, **f–h**, **m–o**, **r**, **t** and **5a**, **c**, **d**, **f–k**, **m–o**, **r**, **s**, **u**in solvent mixtures of specified percentages) and/or usage of crystallization was used in the purification method (**4b**, **e**, **l**, or **p**). It was then dried in a 60 °C vacuum oven or vacuum desiccator with the aid of phosphorus pentoxide (Scheme 1). The structures of compounds were verified by ^{1}H NMR, ^{13}C NMR, IR, elemental, and X-ray diffraction analysis.

Spectral data of synthesized compounds

(4-methylphenyl)methylidenehydrazino-5H-chromeno[4,3-d]pyrimidine-5-ol, 4a. Color: yellow, yield: 11%, m.p.: 251–253 °C. IR (cm^{-1}): 3212.6 (NH), 2926.3 (C–H),

1570.9–1590.9 (C=N), 1532.1–1438.0 (C–O). ^{1}H NMR (400 MHz, DMSO–d_6) δ: 11.37 (s, 1H, OH), 8.49 (s, 1H, NCHC), 8.22–7.08 (m, 9H, Ar-H), 7.61 (s, 1H, CNHN), 6.44–6.46 (d, 1H, OCHOHC), 2.34 (s, 3H, CH_3). ^{13}C NMR (100 MHz, DMSO–d_6) δ: 161.29, 156.82, 154.86, 154.31, 147.79, 139.20, 133.54, 128.97, 128.77, 126.39, 124.89, 122.25, 120.10, 118.46, 116.71, 91.21 (OCHOHC), and 14.11 (CH_3). Anal. Calcd. for $C_{19}H_{15}N_4O_2$ (331.346 g/mol): C: 68.87; H: 4.56; and N: 16.91. Found: C: 68.62; H: 4.51; and N: 16.87.

(4-methylphenyl)methylidenehydrazinopyrimidine-5-yl)(2-hydroxyphenyl) methanone, 5a. Color: yellow, yield: 82%, m.p.: 213–215°C. IR (cm^{-1}): 3222.2 (NH), 3049.7–2871.8 (C-H), 1600.8 (C=O), 1579.6 (C=N). ^{1}H NMR (400 MHz, DMSO-d_6) δ: 11.89 (s, 1H, OH), 10.41 (s, 1H, NH), 8.72 (ss, 2H, NCHCCHNC), 8.22 (s, 1H, CCHNNHC), 6.94–7.61 (m, 8H, Ar-*H*), 2.33 (s, 3H, CH_3). ^{13}C NMR (100 MHz, DMSO-d_6) δ: 192.89 (C=O), 160.89, 160.74, 156.78, 145.59, 139.93, 133.91, 132.24, 130.85, 129.90, 127.27, 124.96, 122.96, 119.90, 117.18, and 21.47 (CH_3). Anal. Calcd. for $C_{19}H_{16}N_4O_2$ (332.354 g/mol): C: 68.66; H: 4.85; and N: 16.86. Found: C: 68.68; H: 4.81; and N: 16.82.

In vitro cytotoxic activity studies of compounds

Cytotoxic activity studies were done according to the literature procedures.[61] HepG2 and MDA-MB-231, which were purchased from the American Type Culture Collection (ATCC, Manassas, VA), were maintained in DMEM medium containing 10% foetal bovine serum and 1% glutaMAX. The cells were seeded into sterile 96-well plates at a density of 4×10^3 cells/well. After 24 h, cells were exposed to drug candidates at concentrations ranging from 200 to 5 μM (200, 100, 50, 20, 10, and 5 μM) for 48 h. 50 μL of MTT stock solution (5 mg/mL) was added to each well after 48 h and the plates were incubated for another 3 h in an incubator. Finally, DMSO (200 μL) was put to each well. Absorbance values were read with the Promega reader device at 560 nm.

Docking studies

An important method used to calculate the theoretical biological activities of molecules against enzymes is molecular docking. In the calculations made by molecular docking method, many parameters are obtained to compare the biological activities of molecules.[62,63] These parameters are very important parameters to explain the theoretical biological activities of molecules. Many enzymes were used to calculate the biological activity of new pyrimidine-chromeno hybrid derivatives. Enzymes used for new pyrimidine-chromeno hybrid derivatives in this study crystal structure of the BRCT repeat region from the breast cancer associated protein, 1JNX,[64] crystal structure of VEGFR kinase (liver cancer) protein, 3WZE,[65] and crystal structure of an allosteric Eya2 phosphatase inhibitor (lung cancer) protein, 5ZMA,[66] was used.

Molecular docking calculations to calculate the biological activity of new pyrimidine-chromeno hybrid derivatives were performed using the Maestro Molecular modeling platform (version 12.2) by Schrödinger. Proteins and new pyrimidine-chromeno hybrid derivatives molecule should be prepared for calculations using the Maestro Molecular

modeling platform (version 12.2) by Schrödinger program. In docking calculations, each stage is completed by different processes for molecules and enzymes. Firstly, it was used from Gaussian software program[67] to obtain optimized structures of molecules. Using these optimized structures, all calculations were made with the Maestro Molecular modeling platform (version 12.2) by Schrödinger, LLC.[68] The Maestro Molecular modeling platform (version 12.2) by Schrödinger comes together from many modules. In the first module between these modules, the protein preparation module [69,70] is used to prepare the enzymes formed by proteins for calculations. In the next module, the LigPrep module[71,72] was used to prepare the new pyrimidine-chromeno hybrid derivatives for calculations.

In the next module, the Glide ligand docking module[73] was used to interact with the molecule and enzymes. OPLS3e method was used in all calculations for docking calculations of molecules and proteins in all modules used. After the docking calculations, ADME/T analysis was performed to examine the future drug properties of the molecule. The Qik-prop module[74] of the Schrödinger software was used for ADME/T analysis.

X-ray diffraction analysis studies

Suitable crystals of **4l** and **5d** were selected for data collection which was performed on a D8-QUEST diffractometer equipped with graphite-monochromatic Mo-K_α radiation at 296 K. The structure was solved by direct methods using SHELXS-2013[75] and refined by full-matrix least-squares methods on F^2 using SHELXL-2013.[76] All nonhydrogen atoms were refined with anisotropic parameters. For **4l** compound; the hydroxyl H atom was in a difference map refined freely. The other H atoms were located from different maps and then treated as riding atoms with C-H distances of 0.93–0.96 Å and N-H distances of 0.86 Å. For **5d** compound; the H atoms were located from different maps and then treated as riding atoms with C-H distances of 0.93–0.96 Å, N-H distance of 0.86 Å, and O-H distance of 0.82 Å. The following procedures were implemented in our analysis: data collection: Bruker APEX2;[77] a program used for molecular graphics: MERCURY programs;[78] the software used to prepare material for publication: WinGX.[79] Details of data collection and crystal structure determinations are given in Tables 3 and 4, respectively.

Crystallographic data for the structural analyses have been deposited with the Cambridge Crystallographic Data Center, CCDC No. 1878421 for compound **4l** and CCDC No. 1900837 for compound **5d**. Copies of this information may be obtained free of charge from the Director, CCDC, 12 Union Road, Cambridge CB2 1EZ, UK (fax: +44-1223-336033; e-mail: deposit@ccdc.cam.ac.uk or www: http://www.ccdc.cam.ac.uk).

^{1}H NMR, ^{13}C NMR, IR spectra, X-ray data and full characterization data of all compounds can be found via the "Supplementary File" section of this article's webpage.'

Acknowledgments

This work was financially supported by the Research Fund of Erciyes Üniversitesi [FDK-2016-6664]. The authors acknowledge the Scientific and Technological Research Application and Research Center, Sinop University, Turkey, for the use of the Bruker D8 QUEST diffractometer.

This research was made possible by TUBITAK ULAKBIM, High Performance and Grid Computing Center (TR-Grid e-Infrastructure).

Disclosure statement

No potential conflict of interest was reported by the author(s).

Funding

This work was financially supported by Erciyes University Research Fund [FDK-2016-6664].

ORCID

Senem Akkoç http://orcid.org/0000-0002-1260-9425

References

[1] Martins, P.; Jesus, J.; Santos, S.; Raposo, L. R.; Roma-Rodrigues, C.; Baptista, P. V.; Fernandes, A. R. *Molecules.* **2015**, *20*, 16852–16891. DOI: 10.3390/molecules200916852.
[2] Amir, M.; Javed, S. A.; Kumar, H. *Indian J. Pharm. Sci.* **2007**, *69*, 337. DOI: 10.4103/0250-474X.34540.
[3] Sahu, M.; Siddiqui, N. *Int. J. Pharm. Pharm. Sci.* **2016**, *8*, 8.
[4] Akkurt, M.; Sarıpınar, E.; Öztürk, S.; Yılmaz, Ç.; Fun, H. K. *Z. Kristallogr.* **2003**, *218*, 488. DOI: 10.1524/zkri.218.7.488.20712.
[5] Önal, Z.; Sanpinar, E.; ILhan, I. Ö. *J. Heterocycl. Chem.* **2001**, *38*, 397–402. DOI: 10.1002/jhet.5570380214.
[6] Joule, A. J.; Smith, G. F. *Heterocyclic Chemistry*; Van Nostrand Reinhold Company: London-England, 1978.
[7] Sukach, V. A.; Tkachuk, V. M.; Rusanov, E. B.; Roschenthaler, G. V.; Vovk, M. V. *Tetrahedron.* **2012**, *68*, 8408–8415. DOI: 10.1016/j.tet.2012.07.099.
[8] Gondkar, A. S.; Deshmukh, V. K.; Chaudhari, S. R. *Drug Invent. Today.* **2013**, *5*, 175–181. DOI: 10.1016/j.dit.2013.04.004.
[9] Çalış, U.; Köksal, M. *Arzneimittelforschung.* **2001**, *51*, 523. DOI: 10.1055/s-0031-1300075.
[10] Saladino, R.; Ciambecchini, U.; Maga, G.; Mastromarino, P.; Conti, C.; Botta, M. *Bioorg. Med. Chem.* **2002**, *10*, 2143–2153. DOI: 10.1016/s0968-0896(02)00077-9.
[11] Gößnitzer, E.; Feierl, G.; Wagner, U. *Eur. J. Pharm.* **2002**, *15*, 49–61. DOI: 10.1016/s0928-0987(01)00202-0.
[12] Ram, V. J.; Haque, N. *ChemInform.* **2010**, *26*, 167.
[13] Prabakaran, P.; Robert, J. J.; Muthiah, P. T.; Bocelli, G.; Righi, L. *Acta Crystallogr. C Cryst. Struct. Commun.* **2001**, *57*, 459–461. DOI: 10.1107/s0108270101000269.
[14] Kumar, R.; Nath, M.; Tyrrell, D. J. *J. Med. Chem.* **2002**, *45*, 2032–2040. DOI: 10.1021/jm010410d.
[15] Martynov, I. Y.; Barachevsky, V. A.; Ayt, A. O.; Kobeleva, O. I.; Valova, T. M.; Levchenko, K. S.; Yarovenko, V. N.; Krayushkin, M. M. *Opt. Mater.* **2014**, *37*, 488–492. DOI: 10.1016/j.optmat.2014.07.011.
[16] Nawrot-Modranka, J.; Nawrot, E.; Graczyk, J. *Eur. J. Med. Chem.* **2006**, *41*, 1301. DOI: 10.1016/j.ejmech.2006.06.004.
[17] Horton, D. A.; Bourne, G. T.; Smythe, M. L. *Chem. Rev.* **2003**, *103*, 893. DOI: 10.1021/cr020033s.

[18] Wang, B.; Yang, Z. Y.; Li, T. *Bioorg. Med. Chem.* **2006**, *14*, 6012–6021. DOI: 10.1016/j.bmc.2006.05.015.
[19] Opretzka, L. C. F.; do Espírito-Santo, R. F.; Nascimento, O. A.; Abreu, L. S.; Alves, I. M.; Döring, E.; Soares, M. B. P.; Velozo, E. D. S.; Laufer, S. A.; Villarreal, C. F. *Int. Immunopharmacol.* **2019**, *72*, 31–39. DOI: 10.1016/j.intimp.2019.03.044.
[20] Jiang, Y. Y.; Guo, F. X.; Chen, L. X.; Xu, L. L.; Zhang, W.; Liu, B. *Fitoterapia.* **2019**, *135*, 114. DOI: 10.1016/j.fitote.2019.04.012.
[21] Demetgül, C.; Beyazit, N. *Carbohydr. Polym.* **2018**, *181*, 812. DOI: 10.1016/j.carbpol.2017.11.074.
[22] Walenzyk, T.; Carola, C.; Buchholz, H.; König, B. *Tetrahedron.* **2005**, *61*, 7366–7377. DOI: 10.1016/j.tet.2005.05.081.
[23] Boumendjel, A.; Nicolle, E.; Moraux, T.; Gerby, B.; Blanc, M.; Ronot, X.; Boutonnat, J. *J. Med. Chem.* **2005**, *48*, 7275–7281.
[24] Lee, K. S.; Seo, S. H.; Lee, Y. H.; Kim, H. D.; Son, M. H.; Chung, B. Y.; Lee, J. Y.; Jin, C.; Lee, Y. S. *Bioorg. Med. Chem. Lett.* **2005**, *15*, 2857–2860. DOI: 10.1016/j.bmcl.2005.03.095.
[25] Huang, W.; Liu, M. Z.; Li, Y.; Tan, Y.; Yang, G. F. *Bioorg. Med. Chem.* **2007**, *15*, 5191. DOI: 10.1016/j.bmc.2007.05.022.
[26] Mays, J. R.; Hill, S. A.; Moyers, J. T.; Blagg, B. S. *Bioorg. Med. Chem.* **2010**, *18*, 249. DOI: 10.1016/j.bmc.2009.10.061.
[27] Zhang, S.; Ma, J.; Bao, Y.; Yang, P.; Zou, L.; Li, K.; Sun, X. *Bioorg. Med. Chem.* **2008**, *16*, 7127–7132. DOI: 10.1016/j.bmc.2008.06.055.
[28] Nam, D. H.; Lee, K. Y.; Moon, C. S.; Lee, Y. S. *Eur. J. Med. Chem.* **2010**, *45*, 4288–4292. DOI: 10.1016/j.ejmech.2010.06.030.
[29] Singh, P.; Kaur, M.; Holzer, W. *Eur. J. Med. Chem.* **2010**, *45*, 4968. DOI: 10.1016/j.ejmech.2010.08.004.
[30] Huang, W.; Ding, Y.; Miao, Y.; Liu, M. Z.; Li, Y.; Yang, G. F. *Eur. J. Med. Chem.* **2009**, *44*, 3687. DOI: 10.1016/j.ejmech.2009.04.004.
[31] Gaspar, A.; Reis, J.; Fonseca, A.; Milhazes, N.; Vina, D.; Uriarte, E.; Borges, F. *Bioorg. Med. Chem. Lett.* **2011**, *21*, 707–707. DOI: 10.1016/j.bmcl.2010.11.128.
[32] Piao, L. Z.; Park, H. R.; Park, Y. K.; Lee, S. K.; Park, J. H.; Park, M. K. *Chem. Pharm. Bull.* **2002**, *50*, 309–311. DOI: 10.1248/cpb.50.309.
[33] Keri, R. S.; Budagumpi, S.; Pai, R. K.; Balakrishna, R. G. *Eur. J. Med. Chem.* **2014**, *78*, 340. DOI: 10.1016/j.ejmech.2014.03.047.
[34] Shim, Y. S.; Kim, K. C.; Chi, D. Y.; Lee, K.; Cho, H. *Bioorg. Med. Chem. Lett.* **2003**, *13*, 2561–2563. DOI: 10.1016/s0960-894x(03)00479-7.
[35] Gasparova, R.; Lácová, M. *Molecules* **2005**, *10*, 937. DOI: 10.3390/10080937.
[36] Habibi, D.; Shamsian, A. *J. Chem. Res.* **2013**, *37*, 253–255. DOI: 10.3184/174751913X13639572643562.
[37] Niknam, K.; Piran, A. *Curr. Opin. Green Sustain. Chem.* **2013**, *3*, 1–8. DOI: 10.4236/gsc.2013.32A001.
[38] El-Sayed Ali, T.; Ibrahim, M. A.; El-Gohary, N. M.; El-Kazak, A. M. *Eur. J. Chem.* **2013**, *4*, 311. DOI: 10.5155/eurjchem.4.3.311-328.815.
[39] Ryabukhin, S. V.; Plaskon, A. S.; Volochnyuk, D. M.; Pipko, S. E.; Tolmachev, A. A. *Heterocycles.* **2008**, *75*, 583. DOI: 10.3987/COM-07-11240.
[40] Lowe, W. *Synthesis.* **1976**, *4*, 274. DOI: 10.1055/s-1976-24020.
[41] Borrell, J. I.; Teixido, J.; Schuler, E.; Michelotti, E. *Tetrahedron Lett.* **2001**, *42*, 5331–5334. DOI: 10.1016/S0040-4039(01)00999-6.
[42] Bruno, O.; Brullo, C.; Ranise, A.; Schenone, S.; Bondavalli, F.; Barocelli, E.; Ballabeni, V.; Chiavarini, M.; Tognolini, M.; Impicciatore, M. *Bioorg. Med. Chem. Lett.* **2001**, *11*, 1397–1400. DOI: 10.1016/S0960-894X(01)00221-9.
[43] Harnisch, H. *Justus Liebigs Ann. Chem.* **1973**, *765*, 8–14. DOI: 10.1002/jlac.19727650103.
[44] Nohara, A.; Umetani, T.; Sanno, Y. *Tetrahedron.* **1974**, *30*, 3553–3561. DOI: 10.1016/S0040-4020(01)97034-6.

[45] Akkoç, S.; Tüzün, B.; İlhan, İÖ.; Akkurt, M. *J. Mol. Struct.* **2020**, *1219*, 128582. DOI: 10.1016/j.molstruc.2020.128582.
[46] Genç Bilgiçli, H.; Bilgiçli, A. T.; Günsel, A.; Tüzün, B.; Ergön, D.; Yarasir, M. N.; Zengin, M. *Appl. Organomet. Chem.* **2020**, *34*, e5624. DOI: 10.1002/aoc.5624.
[47] Ojha, L. K.; Tüzün, B.; Bhawsar, J. *J. Bio. Tribocorros.* **2020**, *6*, 1–10. DOI: 10.1007/s40735-020-00336-z.
[48] Douche, D.; Elmsellem, H.; Anouar, E. H.; Guo, L.; Hafez, B.; Tüzün, B.; El Louzi, A.; Bougrin, K.; Karrouchi, K.; Himmi, B. *J. Mol. Liq.* **2020**, *308*, 113042. DOI: 10.1016/j.molliq.2020.113042.
[49] Kısa, D.; Korkmaz, N.; Taslimi, P.; Tuzun, B.; Tekin, Ş.; Karadag, A.; Şen, F. *Bioor. Chem.* **2020**, *101*, 104066–104066. DOI: 10.1016/j.bioorg.2020.104066.
[50] Aktaş, A.; Tüzün, B.; Aslan, R.; Sayın, K.; Ataseven, H. *J. Biomol. Struct. Dyn.* **2020**, *12*, 1–11. DOI: 10.1080/07391102.2020.1806112.
[51] Aktaş, A.; Tüzün, B.; Taşkın Kafa, H. A.; Sayın, K.; Ataseven, H. *Bratisl. Med. J.* **2020**, *121*, 705. DOI: 10.4149/bll_2020_115.
[52] Gedikli, M. A.; Tüzün, B.; Aktaş, A.; Sayın, K.; Ataseven, H. *Bratisl. Med. J.* **2021**, *122*, 101-110.DOI: 10.4149/bll_2021_015.
[53] Türkan, F.; Taslimi, P.; Abdalrazaq, S. M.; Aras, A.; Erden, Y.; Çelebioğlu, H. U.; Tüzün, B.; Ağırtaş, M. S.; Gülçin, İ. *J. Biomol. Struct. Dyn.* **2020**, *4*, 1–10. DOI: 10.1080/07391102.2020.1768901.
[54] Taslimi, P.; Erden, Y.; Mamedov, S.; Zeynalova, L.; Ladokhina, N.; Tas, R.; Tüzün, B.; Sujayev, A.; Sadeghian, N.; Alwasel, S. H. *J. Biomol. Struct. Dyn.* **2020**, *15*, 1–11. DOI: 10.1080/07391102.2020.1763838.
[55] Huseynova, A.; Kaya, R.; Taslimi, P.; Farzaliyev, V.; Mammadyarova, X.; Sujayev, A.; Tüzün, B.; Koçyiğit, Ü. M.; Alwasel, S.; Gülçin, İ. *J. Biomol. Struct. Dyn.* **2020**, *27*, 1–13. DOI: 10.1080/07391102.2020.1811772.
[56] Çelebioğlu, H. U.; Erden, Y.; Hamurcu, F.; Taslimi, P.; Şentürk, O. S.; Özmen, Ü. Ö.; Tüzün, B.; Gülçin, İ. *J. Biomol. Struct. Dyn.* **2020**, *21*, 1–12. DOI: 10.1080/07391102.2020.1792345.
[57] Demir, Y.; Taslimi, P.; Koçyiğit, Ü. M.; Akkuş, M.; Özaslan, M. S.; Duran, H. E.; Budak, Y.; Tüzün, B.; Gürdere, M. B.; Ceylan, M.; et al. *Arch. Pharm.* **2020**, *353*, e2000118. DOI: 10.1002/ardp.202000118.
[58] Lipinski, C. A. *Drug Discov. Today Technol.* **2004**, *1*, 337–341. DOI: 10.1016/j.ddtec.2004.11.007.
[59] Lipinski, C. A.; Lombardo, F.; Dominy, B. W.; Feeney, P. J. *Adv. Drug Deliv. Rev.* **1997**, *23*, 3–25. DOI: 10.1016/S0169-409X(96)00423-1.
[60] Jorgensen, W. J.; Duffy, E. M. *Adv. Drug Deliv. Rev.* **2002**, *54*, 355–366. DOI: 10.1016/s0169-409x(02)00008-x.
[61] Çağlar Yavuz, S.; Akkoç, S.; Sarıpınar, E. *Synth. Commun.* **2019**, *49*, 3198–3209. DOI: 10.1080/00397911.2019.1661481.
[62] Tüzün, B.; Sarıpınar, E. *J. Iran. Chem. Soc.* **2020**, *17*, 985–1000. DOI: 10.1007/s13738-019-01835-8.
[63] Tüzün, B. *Spectrochim. Acta A. Mol. Biomol. Spectrosc.* **2020**, *227*, 117663. DOI: 10.1016/j.saa.2019.117663.
[64] Williams, R. S.; Green, R.; Glover, J. N. *Nat. Struct. Biol.* **2001**, *8*, 838–842. DOI: 10.1038/nsb1001-838.
[65] Okamoto, K.; Ikemori-Kawada, M.; Jestel, A.; von König, K.; Funahashi, Y.; Matsushima, T. *ACS Med. Chem. Lett.* **2015**, *6*, 89–94. DOI: 10.1021/ml500394m.
[66] Anantharajan, J.; Zhou, H.; Zhang, L.; Hotz, T.; Vincent, M. Y.; Blevins, M. A.; Jansson, A. E.; Kuan, J. W. L.; Ng, E. Y.; Yeo, Y. K.; et al. Mol. Cancer *Ther.* **2019**, *18*, 1484–1496. DOI: 10.1158/1535-7163.MCT-18-1239.
[67] Frisch, M. J.; Trucks, G. W.; Schlegel, H. B.; Scuseria, G. E.; Robb, M. A.; Cheeseman, J. R.; Scalmani, G.; Barone, V.; Mennucci, B.; Petersson, G. A.; et al. *Gaussian 09, Revision D.01*; Gaussian, Inc: Wallingford CT, 2009.

[68] Schrodinger, L. Small-Molecule Drug Discovery Suite. 2019.
[69] *Schrödinger Release 2019-4. Protein Preparation Wizard; Epik*; Schrödinger, LLC: New York, NY, 2016; *Impact*; Schrödinger, LLC, New York, NY, 2016; *Prime*; Schrödinger, LLC, New York, NY, 2019.
[70] Friesner, R. A.; Murphy, R. B.; Repasky, M. P.; Frye, L. L.; Greenwood, J. R.; Halgren, T. A.; Sanschagrin, P. C.; Mainz, D. T. *J. Med. Chem.* **2006**, *49*, 6177–6196. DOI: 10.1021/jm051256o.
[71] Sastry, G. M.; Adzhigirey, M.; Day, T.; Annabhimoju, R.; Sherman, W. *J. Comput. Aided. Mol. Des.* **2013**, *27*, 221–234. DOI: 10.1007/s10822-013-9644-8.
[72] *Schrödinger Release 2019-4*. *LigPrep*; Schrödinger, LLC: New York, NY, 2019.
[73] Du, Q.; Qian, Y.; Yao, X.; Xue, W. *J. Biomol. Struct. Dyn.* **2020**, *38*, 625–633. DOI: 10.1080/07391102.2019.1583605.
[74] *Schrödinger Release 2020-1*: *QikProp*; Schrödinger, LLC: New York, NY, 2020.
[75] Sheldrick, G. M. *Acta. Cryst. A.* **2008**, *64*, 112. DOI: 10.1107/S0108767307043930.
[76] Sheldrick, G. M. *Acta Crystallogr. C Struct. Chem.* **2015**, *71*, 3–8. DOI: 10.1107/S2053229614024218.
[77] *APEX2*; Bruker AXS Inc.: Madison Wisconsin USA, **2013**.
[78] Macrae, C. F.; Bruno, I. J.; Chisholm, J. A.; Edgington, P. R.; McCabe, P.; Pidcock, E.; Rodriguez-Monge, L.; Taylor, R.; van de Streek, J.; Wood, P. A. J. Appl. Crystallogr. **2008**, *41*, 466–470. DOI: 10.1107/S0021889807067908.
[79] Farrugia, L. J. J. Appl. Crystallogr. **2012**, *45*, 849–854. DOI: 10.1107/S0021889812029111.